Comparison of the P-wave velocity structure between the ultraslow-spreading Southwest Indian Ridge (SWIR) at 64°30'E and other ultraslow- and slow-spreading ridges

Ana Corbalán[1*], Mladen Nedimović[1], Ingo Grevemeyer[2], Keith Louden[1], and Louise Watremez[3]

[1]Dalhousie University, Halifax, Canada; [2]GEOMAR Helmholtz Centre for Ocean research Kiel, Germany; [3]University of Lille, France; *a.corbalan@dal.ca

EGU General Assembly
Online | 4–8 May 2020

AVERAGE VELOCITY-DEPTH FUNCTIONS AND VELOCITY BOUNDS

We compute two regional P-wave velocity profiles, one along and one across the eastern Southwest Indian Ridge (SWIR) at 64°30'E, using first arrival travel time tomography (TOMO2D; Korenaga et al., 2000). The wide-angle data used as input for inversion were recorded by 32 ocean bottom seismometers (OBSs). Please see Study Area and Fig. 1 for more details. We interpret the changes in velocity with depth to be related to the degree of serpentinization and the subsurface structure to be composed of highly fractured and fully serpentinized peridotites at the top with a gradual transition to unaltered peridotites at depth (Corbalan et al., 2019).

Next, we extract 1D velocity-depth functions every 1 km along the 2D velocity models in the areas with high ray coverage and a standard deviation of 50-100 m/s, which are the areas with crossing rays and OBSs on the seafloor. We then compute and compare the average 1D velocities and velocity field envelopes with the velocity envelopes from other ridge-normal (Fig. 2a, 2d, 2e, 2f) and ridge-parallel seismic profiles (Fig. 2g–2i) at ultraslow-spreading ridges. We also compare our results with compiled velocity fields of the slow-spreading Mid-Atlantic Ridge (MAR) at segment ends (Grevemeyer et al., 2018a; Fig. 2b and Fig. 2c) and at young crustal ages (White et al., 1992; Fig. 2b and Fig. 2c).

The velocity fields at the SWIR at 66°E (Fig. 2d) and from Momoh et al. (2017) (Fig. 2a) within our study area show an overall agreement with our velocity field envelope. The velocity-depth field envelope from the ultraslow-spreading Mid-Cayman Spreading Center (MCSC; Fig 2a) is comparable to our NS velocities. Like the SWIR in our study area (Fig. 1), the MCSC shows exhumed serpentinized mantle domains (Grevemeyer et al., 2018b). However, the velocity compilations of the MAR (Fig. 2b and 2c) are at shallower depths higher and at greater depths lower than our velocities. This is consistent with the expected structure of young lithosphere at slow-spreading ridges, where igneous crust of normal thickness with distinct upper and lower crust is generally imaged, except at the segment ends where the lower crust is thinner or may be missing.

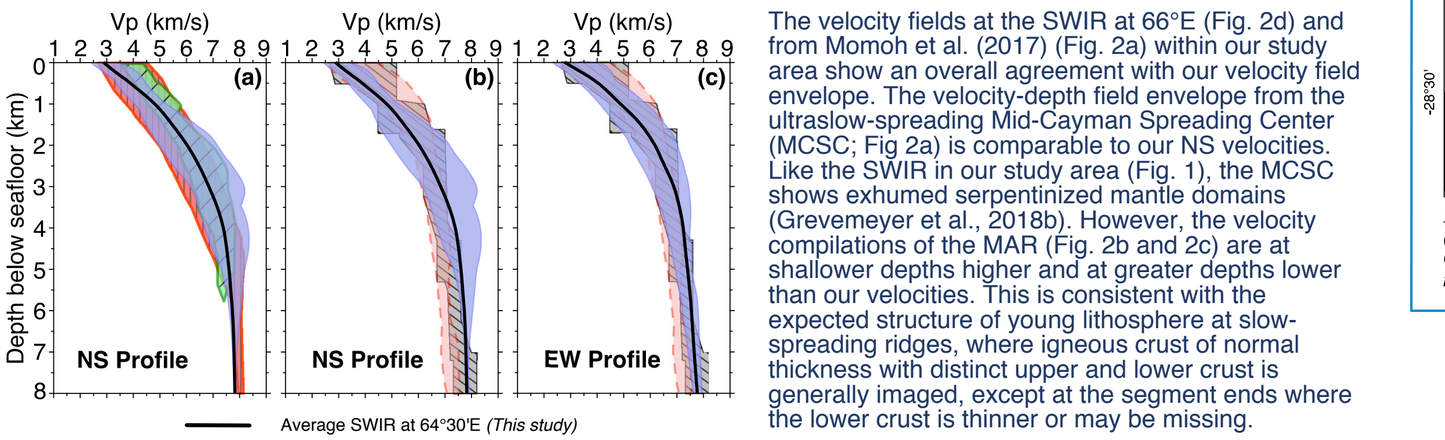

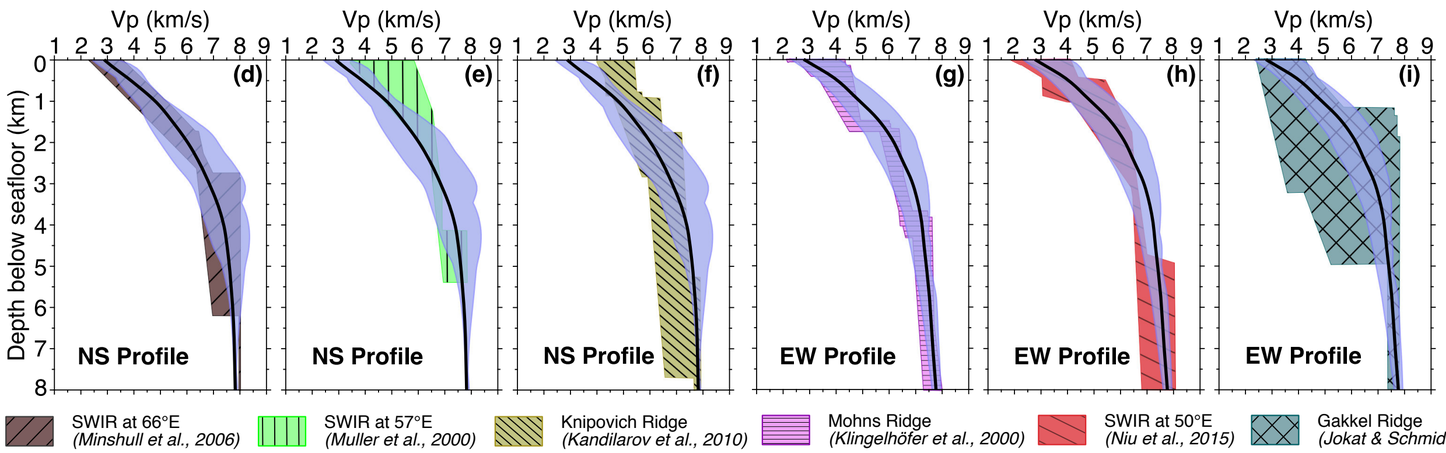

Figure 2. *Comparison of the average velocities and velocity envelopes at the SWIR at 64°30'E with other ultraslow- and slow-spreading ridges. See the text for details.*

Mohns Ridge velocities (Fig. 2g) overall fit within our SWIR velocity field envelope, after taking into account the differences in the modelling approach. Klingelhöfer et al (2000) suggest a very thin and variable thickness lower crust and a normal thickness Layer 2. However, the similarities with our SWIR velocities open up the possibility for an alternative interpretation of the Mohns Ridge velocity structure in terms of serpentinized peridotites. Knipovich Ridge (Fig. 2f) and the SWIR at 57°E (Fig. 2e) and at 50°E (Fig. 2h) show velocities not akin to our velocities. This is expected as these studies extend over segment centers, fracture zones and non-transform discontinuities. They all have reportedly an igneous crust, in some cases even thicker than normal oceanic crust (Fig. 2h). Gakkel velocities (Fig. 2i) show an extremely wide range of velocities making the overlap with our velocities not conclusive.

The comparison between the computed average 1D velocities and velocity field envelopes at the SWIR at 64°30'S and other ultraslow- and slow-spreading ridges, confirms our interpretation of the lithospheric structure at the SWIR, which differs significantly from the lithosphere formed at faster-spreading ridges. Yet more dense OBS seismic profiles, especially at the Arctic ridges, are needed for a more comprehensive comparison.

STUDY AREA

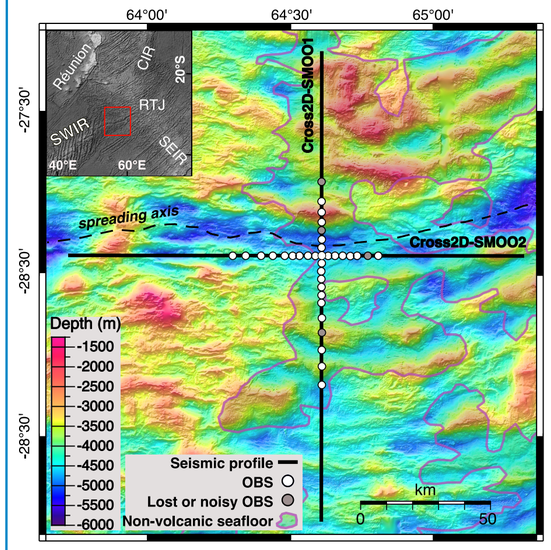

Figure 1. *Bathymetric map (Cannat et al., 2006; Momoh et al., 2017) with the location of the OBS profiles Cross2D-SMOO1 (NS) and Croos2D-SMOO2 (EW). Inset in the top left shows the location of the SWIR relative to the Réunion Island, the Central Indian Ridge (CIR), the Southeast Indian Ridge (SEIR), and the Rodriguez Triple Junction (RTJ). Red square shows the limits of the study area presented in the main figure.*

The easternmost SWIR at 64°30'E is an ultraslow-spreading ridge with a full spreading rate of <14mm/year (Kreemer et al., 2014), where broad domains of non-volcanic seafloor have been identified (Cannat et al., 2006; Fig. 1). Retrieved rock samples indicate this seafloor is primarily constituted of variably serpentinized peridotites (Roumejón et al., 2015).

Coincident multichannel seismic and wide-angle OBS data were collected over two orthogonal 2D ~150km-long-profiles (Fig. 1) during the SISMOMOOTH Survey (Leroy et al., 2015). One profile lies perpendicular to the ridge axis (Cross2D-SMOO1) and the other runs sub-parallel to the axis (Cross2D-SMOO2). The profiles extend mainly over non-volcanic seafloor.

REFERENCES

Cannat, M., Sauter, D., Mendel, V., Ruellan, E., Okino, K., Escartin, J., *et al.* (2006). *Geology*, *34*(7); **Corbalán**, A., Nedimović, M.R., Grevemeyer, I., Watremez, L., & Louden, K.E. (2019) Abstract T12C-03 Paper presented at the 2019 AGU, San Francisco, CA, 9–13 Dec; **Grevemeyer**, I., Ranero, C. R., & Ivandic, M. (2018a). *Geosphere*, *14*(2); **Grevemeyer**, I., Hayman, N.W., Peirce, C., *et al.* (2018b). *Nat. Geosci., 11*; **Jokat**, W., & Schmidt-Aursch, M. C. (2007). *Geophys. J. Int.*, *168*; **Kandilarov**, A., Landa., H., Mjedle, R., Pedersen, R.B., Okin, K., & Murai., Y. (2010). *Mar. Geophys. Res.*, 31; **Klingelhöfer**, F., Géli, L., Matias, L., Steinsland, N., & Mohr, J. (2000). *Geophys. J. Int.*, *141*(2); **Kreemer**, C., Blewitt, G., and Klein, E. C. (2014). *Geochem. Geophys. Geosyst.*, *15*; **Korenaga**, J., Holbrook, W. S., Kent, G. M., Kelemen, P. B., Detrick, R. S., Larsen, H.-C., et al. (2000). *J. Geophys. Res.*, *105*; **Leroy**, S., Cannat, M., Momoh, E., Singh, S., Watremez, L., Sauter, *et. al.* (2015). Abstract V21A-3027 Paper presented at the 2015 AGU, San Francisco, CA, 14–18 Dec; **Minshull**, T. A., Muller, M. R., & White, R. S. (2006). *Geophys. J. Int.l*, *166*(1); **Momoh**, E., Cannat, M., Watremez, L., Leroy, S., & Singh, S. C. (2017). *J. Geophys. Res. Solid Earth*, *122*(12); **Muller**, M. R., Minshull, T. A., & White, R. S. (2000). *J. Geophys. Res.*, *105*(B11); **Niu**, X., Ruan, A., Li, J., Minshull, T. A., Sauter, D., Wu, Z., Qiu, X., Zhao, M., Chen, Y. J., & Singh, S.C. (2015). *Geochem. Geophys. Geosyst.*, *16*; **Roumejon**, S., Cannat, M., Agrinier, P., Godard, M., & Andreani, M. (2014). *J. Petrol.*, *56*(4); **White**, R. S., McKenzie, D., & O'Nions, R. K. (1992). *J. Geophys. Res.*, *97*(B13);

ACKNOWLEDGEMENTS

This work was supported by "la Caixa" Foundation [Scholarship LCF/BQ/AN15/10380004] and by NSERC CREATE TOSST (NSERC Collaborative Research and Training Experience for the Transatlantic Ocean System Science and Technology). We are grateful to the SISMOSMOOTH Cruise Party and the multiple funding partners of the survey.